ELSEVIER

Journal of Biomechanics 40 (2007) 2053–2062

JOURNAL OF BIOMECHANICS

www.elsevier.com/locate/jbiomech
www.JBiomech.com

Mechanics and deformation of the nucleus in micropipette aspiration experiment

Ashkan Vaziri[a,*], Mohammad R. Kaazempur Mofrad[b,**]

[a]*Division of Engineering and Applied Sciences, Harvard University, Cambridge, MA 02138, USA*
[b]*Department of Bioengineering, University of California, Berkeley, CA 94720-1762, USA*

Accepted 27 September 2006

Abstract

Robust biomechanical models are essential for the study of nuclear mechanics and deformation and can help shed light on the underlying mechanisms of stress transition in nuclear elements. Here, we develop a computational model for an isolated nucleus undergoing micropipette aspiration. Our model includes distinct components representing the nucleoplasm and nuclear envelope. The nuclear envelope itself comprises three layers: inner and outer nuclear membranes and one thicker layer representing the nuclear lamina. The nucleoplasm is modeled as a viscoelastic Maxwell material with a single time constant, while a modified Maxwell model, equivalent to a spring and a dashpot in series and both in parallel with a spring, is adopted for the inner and outer nuclear membranes. The nuclear envelope layer is taken as a linear elastic material. The proposed computational model, validated using experimental observations of Guilak et al. [2000. Viscoelastic properties of the cell nucleus. Biochemical and Biophysical Research Communications 269, 781–786] and Deguchi et al. [2005, Flow-induced hardening of endothelial nucleus as an intracellular stress-bearing organelle. Journal of Biomechanics 38, 1751–1759], is employed to study nuclear mechanics and deformation in micropipette aspiration and to shed light on the contribution of individual nuclear components on the response. The results indicate that the overall response of an isolated nucleus in micropipette aspiration is highly sensitive to the apparent stiffness of the nuclear lamina. This observation suggests that micropipette aspiration is an effective technique for examining the influence of various kinds of alteration in the nuclear lamina, such as mutations in the gene encoding lamin A, and also structural remodeling due to mechanical perturbation.

Keywords: Nuclear mechanics; Micropipette aspiration; Nuclear envelope; Nuclear lamina; Viscoelasticity; Finite element model

1. Introduction

The nucleus is the defining feature of eukaryotic cells. It contains the chromosomes and is a site of major metabolic activities, such as DNA replication, gene transcription, RNA processing and ribosome subunit maturation and assembly. The nucleus is separated from the cytoplasm by the nuclear envelope, which comprises inner and outer nuclear membranes, nuclear pore complexes and nuclear lamina. The inner and outer membranes are each a lipid bilayer separated by a small, electron transparent region of approximately 10–40 nm. The outer nuclear membrane is continuous with the endoplasmic reticulum, or 'rough ER', where the translation of membrane-bound proteins takes place. Thus, the nuclear envelope serves to partition the sites of gene transcription from those of protein synthesis in eukaryotic cells.

The lamina is a polymeric network composed of coiled-coil proteins called lamins (Aebi et al., 1986; McKeon et al., 1986). Lamins play an important role in structural integrity of the nucleus, and as an attachment site for chromatin (Newport and Forbes, 1987). Mammalian cells produce two lamin protein types, referred to as A-type and B-type. A-type lamins, which are further categorized as lamin A, AΔ10 and C are the product of a single gene (*Lmna*) and are expressed mainly in differentiated cells. However, B-type lamins, lamin B1 and B2/B3, are encoded

*Corresponding author. Tel.: +1 617 496 5167; fax: +1 617 495 9837.
**Also Corresponded to. Tel.: +1 510 643 8165; fax: +1 510 642 5835.
E-mail addresses: avaziri@deas.harvard.edu (A. Vaziri), mofrad@berkeley.edu (M.R.K. Mofrad).

0021-9290/$ - see front matter © 2006 Elsevier Ltd. All rights reserved.
doi:10.1016/j.jbiomech.2006.09.023

by two distinct genes (*Lmnb1* and *Lmnb2*) that are expressed ubiquitously and are vital for cell viability and function (Stuurman et al., 1995). Studies have linked mutations in *Lmna* and its binding partners with various diseases, such as Emery–Dreifuss muscular dystrophy, dilated cardiomyopathy, familial partial lipodystrophy and Hutchinson–Gilford progeria syndrome (Bonne et al., 1999; Cao and Hegele, 2000; Eriksson et al., 2003; Fatkin et al., 1999; Muchir et al., 2000).

Micropipette aspiration experiment has been used extensively to evaluate the mechanical behavior of cells and nuclei (for example, see Guilak et al., 2000; Trickey et al., 2000; Deguchi et al., 2005; Rowat et al., 2005; Alexopoulos et al., 2005). The present study continues the effort underway for several years by a number of groups to develop robust biomechanical models for micropipette aspiration experiment (Dischер et al., 1998; Drury and Dembo, 1999; Haidar and Guilak, 2000; Charras et al., 2004; Guilak et al., 2005; Baaijens et al., 2005; Trickey et al., 2006). In this paper, a computational model is developed to study the mechanics of an isolated nucleus undergoing micropipette aspiration. This study will help distinguish the role of different nuclear elements on the biomechanical response of an isolated nucleus. The developed computational model includes separate components representing the nucleoplasm and nuclear envelope. The nuclear envelope itself comprises three layers: inner and outer nuclear membranes and one thicker layer representing the nuclear lamina (Fig. 1a). Similar biomechanical model was developed in Vaziri et al. (2006) for studying the mechanics of an isolated nucleus in AFM indentation.

The details of the proposed computational model is described in Section 2, while Section 3 presents the material models employed to represent the mechanical behavior of nuclear elements. In Section 4, a parametric study is carried out to highlight the role of individual nuclear elements on overall response of an isolated nucleus in micropipette aspiration experiment. In Section 5, the proposed computational model is used to mimic experimental observations from Guilak et al. (2000) on articular chondrocytes isolated nuclei and Deguchi et al. (2005) on endothelial isolated nuclei.

2. Computational model for nuclear mechanics in micropipette aspiration

An axisymmetric model for an isolated nucleus in micropipette aspiration experiment is developed with the radius of 3 μm (Fig. 1b), inspired by the experiments on isolated nuclei of articular chondrocytes (Guilak et al. 2000). The nuclear (inner and outer) membranes and the nuclear lamina have constant thickness of 7.5 and 25 nm, respectively (Senda et al., 2005), i.e. the total thickness of nuclear envelope is 40 nm. In the computational model, the perinuclear space between the inner and outer nuclear membranes is not included due to its relatively structure-free composition (Schatten and Thoman, 1978). The

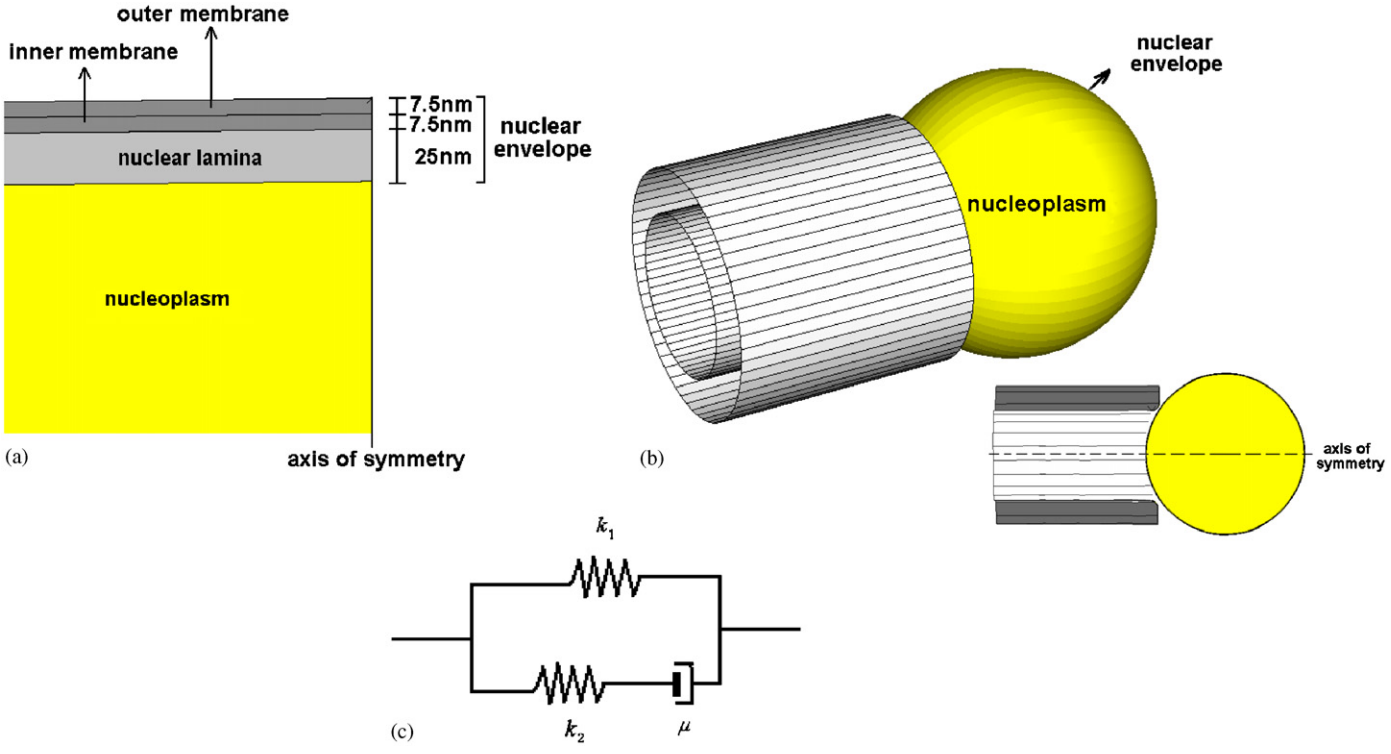

Fig. 1. (a) Nuclear elements considered in the proposed computational model. (b) Computational model of the micropipette aspiration experiment. (c) Material model employed for the inner and outer nuclear membranes. The material model is a modified Maxwell model analogous to a spring and a dashpot in series and both in parallel with a spring.

contact condition between the inner membrane and outer membrane is amongst the uncertainties in the computational model. While the perinuclear space has a relatively structure-free composition, the physical connection between the nuclear lamina and cytoskeleton is related to direct protein connections through this region (Padmakumar et al., 2005; Haque et al., 2006). Another complexity is the numerous nuclear pores lying between the inner and outer nuclear membranes. We will examine the effect of this contact conditions on the overall response of the isolated nucleus (see Section 4). On the other hand, emerin and lamin B receptors (LBR) bind the lamin A/C and lamin B to the inner nuclear membrane, respectively (Ostlund and Worman, 2003; Maraldi et al., 2004). Based on these protein–protein interactions, we assumed no slippage condition between the nuclear lamina and the inner nuclear membrane. Moreover, no slippage is allowed at the interface between the nuclear lamina and the nucleoplasm, consistent with high-resolution micrographs, which provide evidence of direct lamin–chromatin connections (Burke and Stewart, 2002). Free slipping contact is assumed between the nucleus outer membrane and the micropipette walls. A small radius of curvature is introduced at the inner wall edge of the micropipette to help convergence at large deformation in the computational model.

All the consequent computations are performed using a commercially available finite element modeling software ABAQUS/Standard (Hibbit, Karlsson and Sorensen Inc., Providence, RI). Eight-node biquadratic axisymmetric finite elements are employed in calculations for both nucleoplasm and nuclear envelope layers. A mesh sensitivity study is carried out to ensure the independence of the results from the computational mesh.

3. Material models

The nucleoplasm is represented by viscoelastic Maxwell model analogous to a spring and a dashpot in series, which is revealed to be consistent with our experimental findings over a narrow frequency range (Vaziri et al., 2006). The initial stiffness and characteristic time associated with the nucleoplasm material model are denoted by E and τ, respectively. It is postulated that the nucleoplasm behavior in both pure shear and hydrostatic pressure follows this viscoelastic model with a unique characteristic time. The elastic modulus of nucleoplasm in a mouse embryo fibroblast nucleus was approximately $\sim$30 Pa, estimated by interpreting the results of the sharp probe indentation experiment with computational simulations (Vaziri et al., 2006). The results of nanoparticle tracking measurement suggest the elastic modulus of 18 Pa for the nucleoplasm of 3T3 fibroblast nucleus (Tseng et al., 2004). Here, the baseline material constants associated with the Maxwell viscoelastic model for the nucleoplasm are taken to be $E = 30$ Pa and $\tau = 1$ s.

To model the mechanical behavior of the inner and outer membranes, here, we employ a *modified Maxwell model*, analogous to a spring and a dashpot in series and both in parallel with a spring, Fig. 1c. The nuclear lamina is modeled as a linear elastic material and for the sake of simplicity, the strain-hardening behavior of the nuclear lamina is not considered in the present computational model (Panorchan et al., 2004a, b; Dahl et al., 2004; Rowat et al., 2005). In prescribing the material properties, we relied on well-established values for the initial apparent stiffness of lipid bilayers (Mohandas and Evans, 1994; Zhelev et al., 1994; Heinrich et al., 2001), and our own and other published data for the nuclear envelope (Dahl et al., 2004; Vaziri et al., 2006). Based on the reported results, the initial apparent stretching stiffness (defined here simply as product of the initial apparent elastic modulus and the thickness with units of N/m) of *one* lipid bilayer is prescribed as $\kappa_b(t=0) = 16\,\mathrm{mN/m}$ (corresponding to the bending stiffness of $10^{-19}\,\mathrm{N\,m}$ for a 7.5 nm thick lipid bilayer), while the base stretching stiffness of the nuclear lamina is taken as $\kappa_{NL} = 5\,\mathrm{mN/m}$ (which corresponds to the bending stiffness of $3.5\times10^{-19}\,\mathrm{N\,m}$ for a 25 nm thick nuclear lamina). This leads to the total initial stiffness of 37 mN/m for the nuclear envelope. To fully characterize the material behavior of the inner and outer membranes in the current computational model, two more material constants are required: their characteristic time, τ_b, and final apparent stiffness, $\kappa_b(t=\infty)$. The adopted material model for the nuclear elements is consistent with the generalized Maxwell model by Guilak et al. (2000) based on the experimental observations suggested for an articular chondrocytes isolated nucleus. These material models are also consistent with our previous study (Vaziri et al., 2006), where it was shown that the inner and outer membranes behave as elastic materials at time scales significantly smaller than the characteristic time associated with their material model. In this paper, the results are presented with respect to the ratio of the final apparent stiffness to its initial value for the nuclear membranes, denoted by α_b, that is, $\alpha_b = \kappa_b(t=\infty)/\kappa_b(t=0)$.

Both nucleoplasm and nuclear lamina layers are assumed nearly incompressible. Furthermore, it was assumed that the inner and outer membranes behave as linear elastic materials under hydrostatic pressure. In the current study, the Poisson ratio of all the nuclear elements is taken to be 0.48. The role of the nuclear elements Poisson ratio on the overall response of an isolated nucleus in micropipette aspiration experiment will be discussed in Section 4.

4. Numerical results for nuclear mechanics in micropipette aspiration

The geometrical details of computational model employed in this section are depicted in Fig. 2a. In all the calculations presented in this section, the aspiration pressure is ramped linearly to 500 Pa in 10 s and then kept constant. To distinguish the role of the nucleoplasm

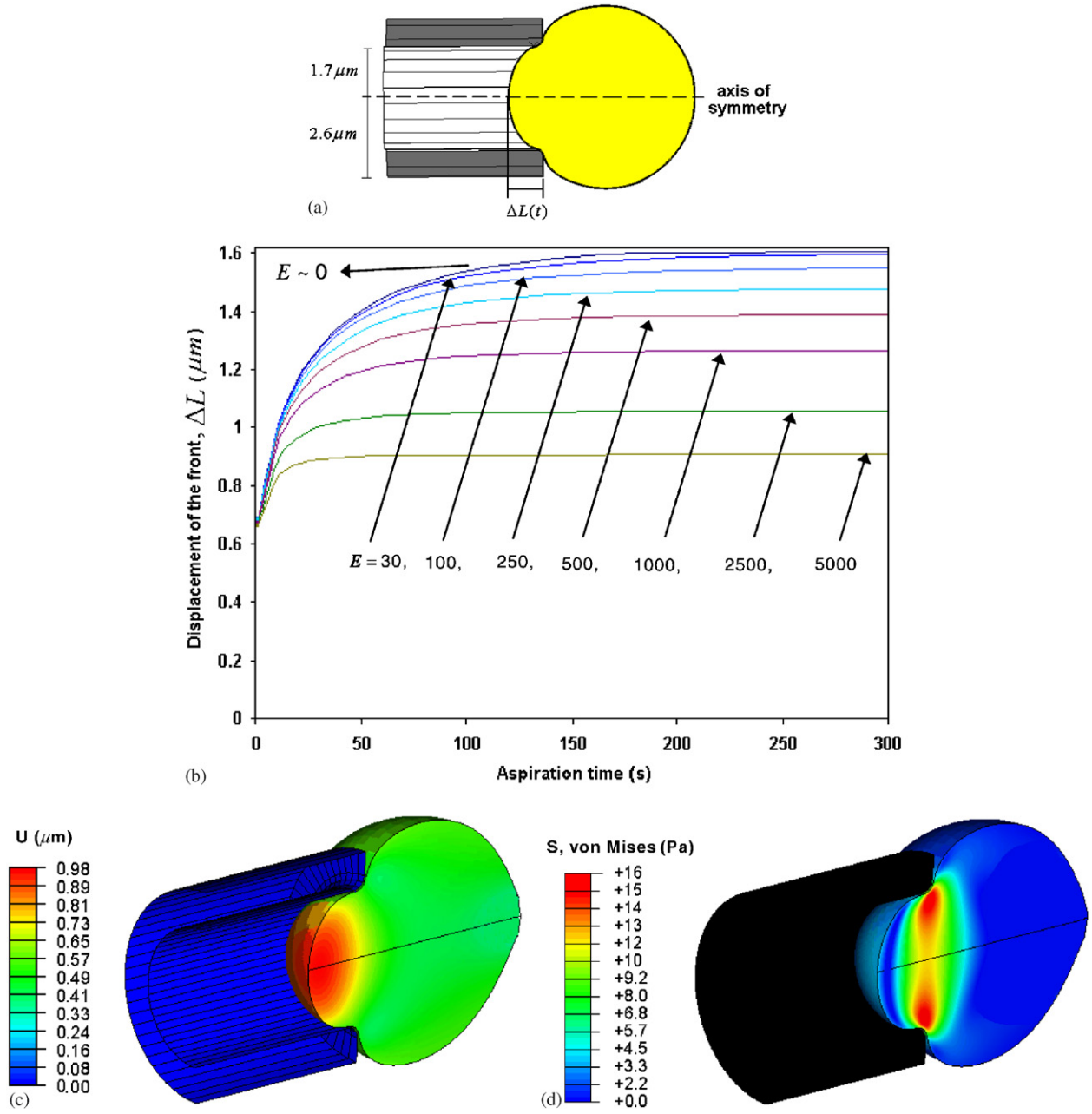

Fig. 2. (a) Geometrical details of the computational model. The nucleus has the radius of 3 μm (average size of an isolated articular chondrocytes nucleus). The inner wall edge of the micropipette has the radius of 0.2 μm. (b) Effect of nucleoplasm elastic modulus on the response of a nucleus under micropipette aspiration. The computations are performed for the following material parameters of the nuclear membrane: $\kappa_{NL} = 5\,mN/m$, $\kappa_b(t=0) = 16\,mN/m$, $\alpha_b = 0.01$ and $\tau_b = 5\,s$. The aspiration pressure is ramped linearly to 500 Pa in 10 s and then kept constant. (c) Displacement field and (d) effective stress (von Mises stress) field in the nucleoplasm having $E = 30\,Pa$ at aspiration time of 300 s.

stiffness on the response of an isolated nucleus in micropipette aspiration, a set of calculations is performed considering the nucleoplasm as a linear elastic material (Fig. 2b). The distribution fields for effective (von Mises) stress and deformation in the nucleoplasm at the aspiration time = 300 s are presented in Figs. 2c and 2d, respectively, for $E = 30\,Pa$. The effective stress field is localized at the vicinity of nuclear membrane contact with the edge of the micropipette. As expected, by employing Maxwell viscoelastic model with a single characteristic time for the nucleoplasm, which is varied between 0.05–5 s, the sensitivity of the overall response under micropipette aspiration to the nucleoplasm stiffness diminishes. Note that this characteristic time is substantially lower than the time course of experiment and the stress field in the nucleoplasm vanishes at early stages of the simulation. Computational analysis is carried out to explore the role of the contact condition between the nuclear envelope layers and also between the

nuclear lamina and the nucleoplasm on the response of an isolated nucleus in micropipette aspiration experiment. No considerable sensitivity to these contact conditions is observed. This implies that the response is mostly dominated by stretching of the nuclear envelope, not its bending. This is in contrast with the sharp probe indentation of the nucleus, where the assumption of no tangential slip at the contacts between the inner and outer nuclear membranes estimates considerably higher required force at a given level of indentation indentation of the nucleus (Vaziri et al., 2006). In all the subsequent calculations, it is assumed that the nuclear (inner and outer) membranes are free to slide relative to each other.

A set of computations is carried out to distinguish the structural role of nuclear envelope layers on the overall response of an isolated nucleus in micropipette aspiration experiment. Fig. 3a displays the role of the final apparent stiffness of the nuclear membranes on the response of an isolated nucleus by varying α_b between 0.01 and 1, where $\alpha_b = 1$ corresponds to the linear elastic behavior.

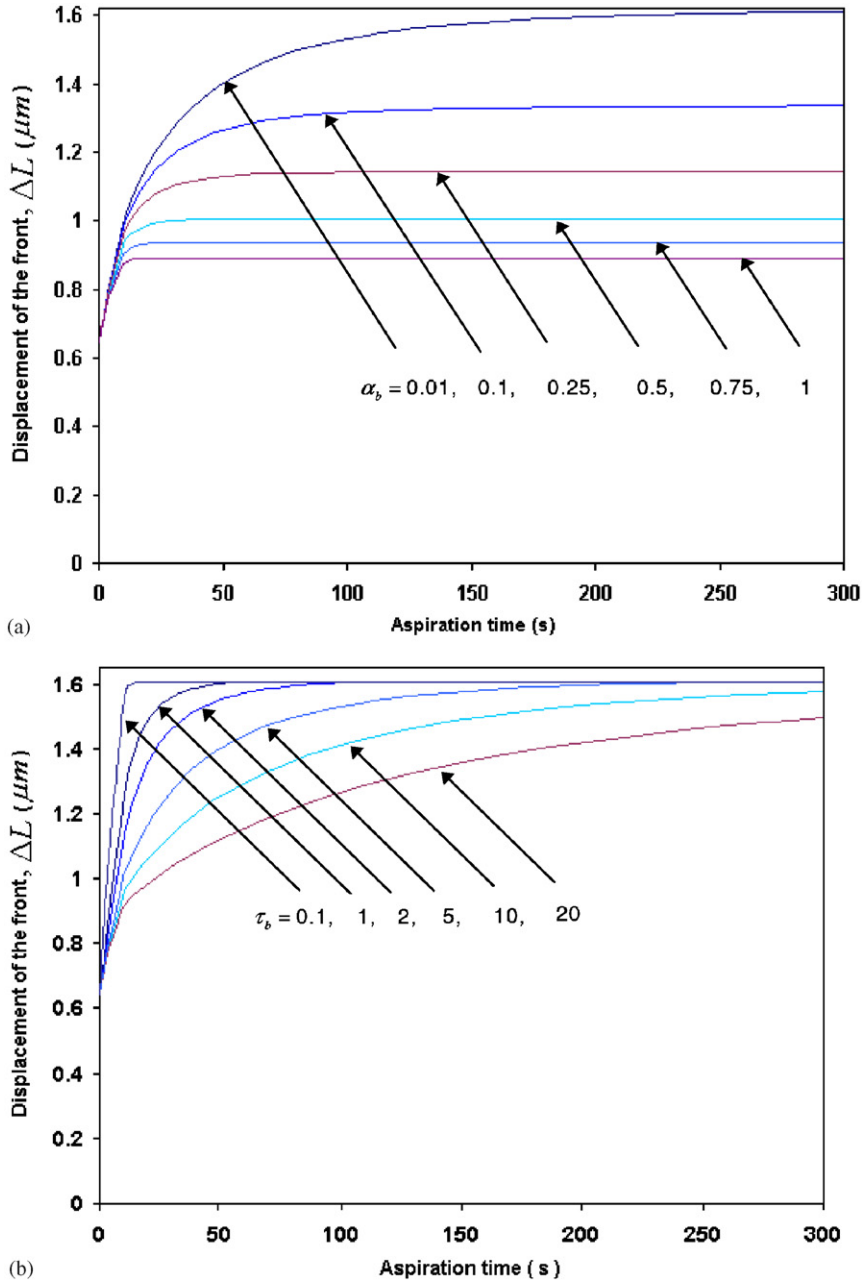

Fig. 3. (a) Effect of the final apparent stiffness of the inner and outer membranes on the response of an isolated nucleus in micropipette aspiration. The characteristic time associated with the viscous element of the nuclear membranes is kept constant as $\tau_b = 5$ s. (b) Dependence of the response of an isolated nucleus in micropipette aspiration on the characteristic time associated with its material model, τ_b. In this set of calculations, $\alpha_b = 0.01$. The computations presented in this figure are performed for the following material parameters: $\kappa_{NL} = 5$ mN/m, $\kappa_b(t = 0) = 16$ mN/m, $E = 30$ Pa and $\tau = 1$ s. The aspiration pressure was ramped linearly to 500 Pa in 10 s and then kept constant. The geometrical detail of the computational model is shown in Fig. 2a.

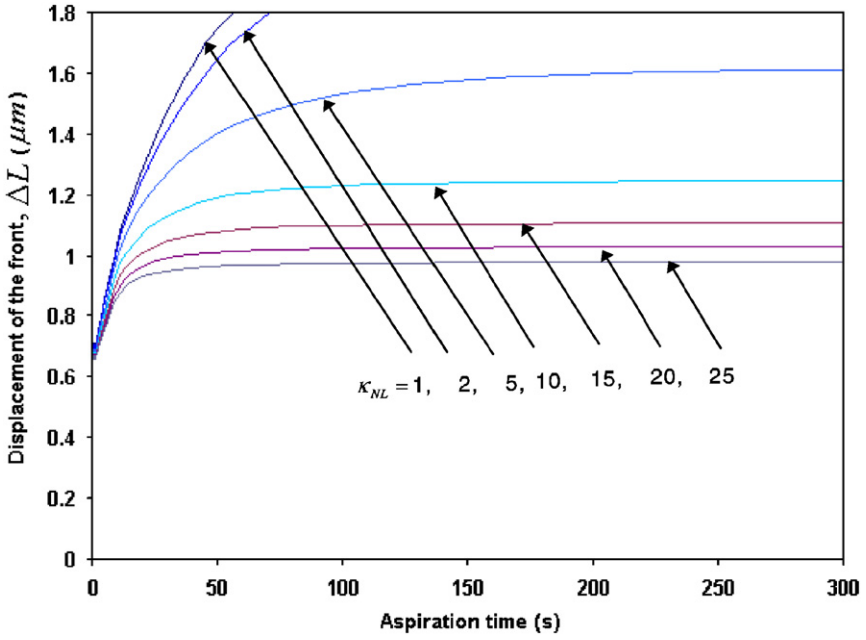

Fig. 4. Effect of the nuclear lamina stiffness on the response of an isolated nucleus to micropipette aspiration. The computations are performed for the following material parameters of the nuclear membrane: $\kappa_b(t=0) = 16\,\mathrm{mN/m}$, $\alpha_b = 0.01$ and $\tau_b = 5\,\mathrm{s}$. The nucleoplasm is modeled as a viscoelastic Maxwell material with $E = 30\,\mathrm{Pa}$ and $\tau = 1\,\mathrm{s}$. The aspiration pressure was ramped linearly to 500 Pa in 10 s and then kept constant. The geometrical detail of the computational model is shown in Fig. 2a.

The dependence of the nucleus response on the characteristic time associated with the nuclear membrane material model is presented in Fig. 3b. The calculations are performed for $E = 30\,\mathrm{Pa}$, $\tau = 1\,\mathrm{s}$, $\kappa_{NL} = 5\,\mathrm{mN/m}$, $\kappa_b(t=0) = 16\,\mathrm{mN/m}$. Furthermore, a set of calculations is carried out to highlight the influence of the nuclear lamina stiffness on the overall response of an isolated nucleus in micropipette aspiration experiment (Fig. 4). In these calculations, the stretching stiffness of the nuclear lamina is varied in the range of 1–25 mN/m, while keeping the following material constants: $\kappa_b(t=0) = 16\,\mathrm{mN/m}$, $\alpha_b = 0.01$, $\tau_b = 5\,\mathrm{s}$, $E = 30\,\mathrm{Pa}$, $\tau = 1\,\mathrm{s}$. The large magnitudes of stretching strain observed here at the site of aspiration in the nuclear membrane are consistent with previous observations on oocyte nuclei (Dahl et al., 2004).

The dependence of the numerical results on the applied pressure is examined by varying the value of maximum applied pressure in the range of 100–600 Pa. The range of aspiration pressure studied here is representative of the range mostly used in the micropipette aspiration experiments (Guilak et al., 2000; Deguchi et al., 2005). The results indicate that the finalized displacement of the front increases approximately linearly as aspiration pressure increases. Furthermore, it is revealed that the overall response of the nucleus to micropipette aspiration is not sensitive to the nucleoplasm Poisson ratio. It should be emphasized that the nucleoplasm behavior under hydrostatic pressure is represented by viscoelastic Maxwell model and it is conceivable that employing other constitutive laws might lead to a contrary conclusion.

5. Comparison with the experimental observations

The results of the proposed computational model are compared with the experimental observations from Guilak et al. (2000) on articular chondrocytes isolated nuclei (see Fig. 5). The readers are referred to Guilak et al. (2000) for details of nuclei isolation and experimental procedures. In the simulations presented in this section, the nucleoplasm is modeled as viscoelastic Maxwell material with $E = 30\,\mathrm{Pa}$ and $\tau = 1\,\mathrm{s}$. To mimic the experimental results, we speculated that the final apparent stiffness of the inner and outer membranes is significantly lower than their initial stiffness and is taken as $\alpha_b = 0.01$, which is consistent with recent observations by Rowat et al. (2006), where it was shown that the nuclear membranes have minimal contribution in the overall stiffness of an isolated nucleus extracted from *HeLa* cells at its final equilibrium stage. Fitting to the experimental results is performed by varying the characteristic time associated with material model of the nuclear membranes and the stretching stiffness of the nuclear lamina. In the computations, the aspiration pressure is ramped linearly to 300 Pa, the average pressure utilized in the experiments, in 10 s and then kept constant. The computational results closely replicate the experimental results for $\kappa_{NL} = 5\,\mathrm{mN/m}$ and $\tau_b = 5\,\mathrm{s}$.

To further validate our model, we set out to simulate the recent micropipette aspiration experiments on isolated endothelial nuclei (Deguchi et al., 2005). In the experiments (see Fig. 6), the micropipettes were coated with poly D-lysine to prevent cellular debris adhesion during the test,

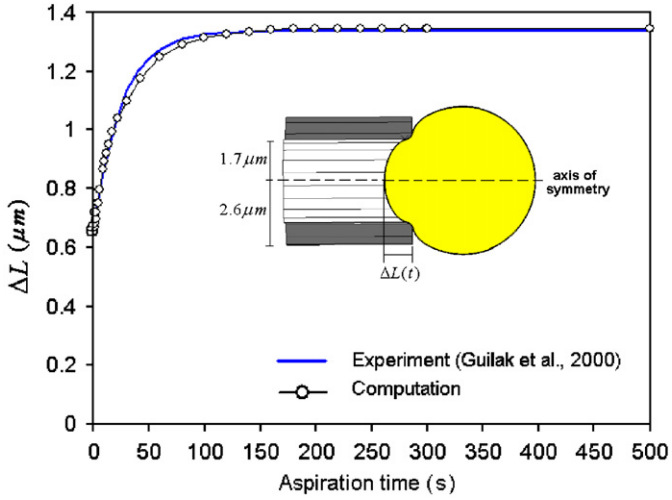

Fig. 5. Comparison of the results of the computational model with the average response of the chemically isolated articular chondrocytes nuclei ($n = 15$) from Guilak et al. (2000). The computational result is presented for the following material parameters of the nuclear envelope: $\kappa_{NL} = 5\,mN/m$, $\kappa_b(t = 0) = 16\,mN/m$, $\alpha_b = 0.01$ and $\tau_b = 5\,s$. The nucleoplasm is modeled as viscoelastic Maxwell material with the baseline material properties: $E = 30\,Pa$ and $\tau = 1\,s$. In the computations, aspiration pressure was increased linearly to 300 Pa in 10 s and then held constant. Inset: the geometrical detail of the computational model.

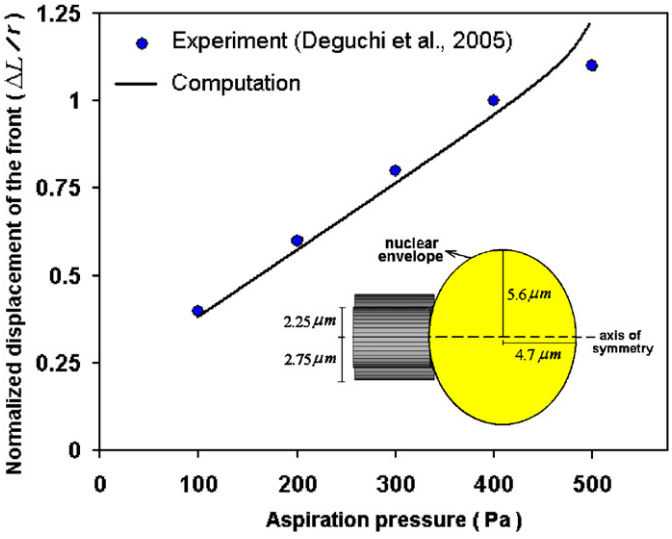

Fig. 6. Comparison of the results of the computational model with the average response of chemically isolated endothelial nuclei ($n = 11$) from Deguchi et al. (2005). The results present the influence of the aspiration pressure on the displacement of the front, normalized by the inner radius of the micropipette, r. The computation results are associated with the following material parameters of the nuclear membrane: $\kappa_b(t = 0) = 16\,mN/m$, $\alpha_b = 0.01$, $\kappa_b = 2.1\,mN/m$. The nucleoplasm is modeled as a viscoelastic Maxwell material with $E = 30\,Pa$ and $\tau = 1\,s$. Inset: geometry of the computational model. The micropipette has the inner and outer radii of 2.25 and 2.75 μm, respectively (average dimensions of the micropipettes used in the experiments). The inner wall edge of the micropipette has the radius of 0.2 μm. The computational model of the isolated endothelial nucleus has an elliptical cross-section with the minor and major axes of 4.7 and 5.6 μm, respectively, consistent with the experimental observation.

which is consistent with the assumption of free slipping contact between the nucleus outer membrane and the micropipette walls. The computational results are presented for the following set of material constants: $\kappa_{NL} = 2.1\,mN/m$, $\kappa_b(t = 0) = 16\,mN/m$ and $\alpha_b = 0.01$, and the baseline properties of the nucleoplasm presented in Section 3. It should be noted that the characteristic time associated with nuclear membrane material model does not alter the final displacement of the nucleus. Both the computational and experimental results clearly display the influence of the aspiration pressure on the displacement of the front, normalized by the inner radius of the micropipette (r).

6. Discussion

Despite the assumptions made for the sake of simplicity, the results presented in Figs. 2–4 highlight the essence of nuclear mechanics and deformation in micropipette aspiration experiment. The finalized displacement of the front is highly sensitive to the final apparent stretching stiffness of the nuclear envelope layers, while it exhibits no dependence on the characteristic time associated with nuclear membrane material model. On the other hand, this characteristic time has a considerable influence on the time history of response.

This study suggests that micropipette aspiration is indeed a robust technique to examine the influence of various kinds of alteration in the nuclear lamina, such as mutation in gene encoding lamin A and its binding and also structural remodeling due to mechanical stresses. Mutations in the genes encoding lamin A and its binding partners have been associated with a variety of human diseases including Emery–Dreifuss muscular dystrophy, dilated cardiomyopathy, limb girdle muscular dystrophy, Dunnigan-type familial partial lipodystrophy and Hutchinson–Gilford progeria syndrome (Bonne et al., 1999; Cao and Hegele, 2000; Eriksson et al., 2003; Fatkin et al., 1999; Muchir et al., 2000). Lamin A/C deficiency and other kinds of mutation may considerably alter the nuclear lamina, jeopardizing the structural integrity of the nucleus (Fidzianska et al., 1998; Hutchison et al., 2001; Lammerding et al., 2004, 2005; Worman and Courvalin, 2004; Wilson, 2005).

In vivo experimental observations show that the endothelial nuclei elongate and orient in the direction of blood flow (Flaherty et al., 1972). Deguchi et al. (2005) recently suggested that not only endothelial cell cytoskeleton but also its nucleus undergo structural remodeling under shear stress applied to the cell. This study suggested that the shear stress applied to the cell may induce structural rearrangement in the structure of its nucleus, which leads to permanent alteration of its overall shape and an increase in its apparent stiffness. This cytoskeleton-mediated deformation of the nucleus appears as a possible mechanotransduction pathway through which shear stress may be transduced to gene-regulating signals (Davies,

1995; Ingber, 1997; Janmey, 1998). The underlying mechanisms of hardening under cytoskeleton-mediated stresses are still ambiguous at this time. One possible explanation is rearrangement of the lamina network as the nucleus is subjected to mechanical stresses (Deguchi et al., 2005). Additional investigations using the proposed computational model can elucidate the underlying mechanisms of this cytoskeleton-mediated hardening of the nucleus, while our preliminary results support the above-mentioned hypothesis.

While we believe the current model to be consistent with most published observations, questions remain regarding the precise nature of the model and its relationship to real nuclear structure. Previous images of isolated nuclei have suggested that in the non-swelled state, the nuclear membrane might be highly folded (Dahl et al., 2004). This might explain the ability of a nucleus to undergo strains of several hundred percent. Another possible explanation is that additional membrane material might be recruited from material that remains attached to the nuclei after isolation. Furthermore, the contribution of the nuclear pore complexes to the mechanical response of the nucleus is neglected in our present model and is subject of future studies. Dense patches of heterochromatin, i.e. condensed form of chromatin organization believed to silence particular genes, are typically present at localized regions in the nucleus just inside the inner nuclear membrane (Dillon, 2004). However, not much is known about their stiffness and contribution to nuclear mechanics. Our model does not consider a separate component for representing the patches of heterochromatin, whose role in the mechanics of the nucleus is not yet well understood. The geometrical distribution, density and stiffness patterns of heterochromatin patches call for more a complex model, which is the subject of our future studies. As shown in Figs. 3 and 4, the penetration depth (displacement of the front) is remarkably sensitive to the stretching stiffness of the nuclear envelope. It is conceivable that inclusion of localized, dense patches of heterochromatin will lead to more complex patterns of penetration depth vs. aspiration pressure. The current model incorporates the overall contribution of a spatially averaged representation of nuclear envelope layers. Interestingly, fitting the computational results to experimental data of Guilak et al. (2000) and Deguchi et al. (2005) shows remarkable agreement and supports the effectiveness of the proposed computational model for modeling the micropipette aspiration experiment. As for the nucleoplasm, while the values used here for shear modulus are consistent with single particle tracking measurements (Tseng et al., 2004), they differ by orders of magnitude from values suggested by other studies of whole-nucleus deformation (Guilak et al., 2000; Caille et al., 2002). Since most of these latter studies neglect the effect of the nuclear membrane and attribute structural integrity exclusively to the nucleoplasm, comparisons between these previously reported values of modulus and the ones used here may not be appropriate.

To highlight and characterize the role of the elastic stiffness of the nucleoplasm on the mechanics of the nucleus, we performed a set of separate calculations wherein the nucleoplasm was modeled as linear elastic (Fig. 2b). In pathological conditions or highly differentiated cell types, it is conceivable that chromatin is hyperproliferated or becomes increasingly condensed or segregated (Pflumm, 2002; Swedlow and Hirano, 2003). Chromatin condensation or segregation, characterized with altered structural motifs in chromosome architecture, can greatly alter the stiffness of the chromatin thereby affecting the nucleoplasm stiffness. As depicted in Fig. 2b, the mechanics of the nucleus and its penetration depth in micropipette aspiration are largely sensitive to nucleoplasm stiffness.

Finally, in the present model, the effects of fluid expulsion from the nucleus are reflected by values of the Poisson ratio that allow for some degree of compressibility. A realistic model of these effects would necessarily have to include fluid leakage through the pores that is both pressure- and time-dependent. Dahl et al. (2005) have recently proposed that the nucleus behaves as a viscoelastic material according to a power-law behavior, as has been found in the cytoskeleton (Fabry et al., 2001). It is conceivable that incorporating the proposed material model for the nucleoplasm would not alter the qualitative results presented here as the stiffness of the nucleoplasm diminishes drastically by time due to the viscous nature of the proposed model (Sollich, 1998; Fabry et al., 2003; Vaziri et al., 2007).

Acknowledgments

We thank Dr. Roger D. Kamm, Dr. John W. Hutchinson, Dr. Zhenyu Xue, Dr. Bashir A. Tafti and Dr. Amy Rowat for fruitful discussions and Neda Movaghar for help with illustrations. This work has been supported in part by the Division of Engineering and Applied Sciences, Harvard University (A.V.) and in part by University of California Regents Fellowship Program (M.R.K.M.).

References

Aebi, U., Cohn, J., Buhle, L., Gerace, L., 1986. The nuclear lamina is a meshwork of intermediate-type filaments. Nature 323, 560–564.

Alexopoulos, L.G., Williams, G.M., Upton, M.L., Setton, L.A., Guilak, F., 2005. Osteoarthritic changes in the biphasic mechanical properties of the chondrocyte pericellular matrix in articular cartilage. Journal of Biomechanics 38, 509–517.

Baaijens, F.P., Trickey, W.R., Laursen, T.A., Guilak, F., 2005. Large deformation finite element analysis of micropipette aspiration to determine the mechanical properties of the chondrocyte. Annals of Biomedical Engineering 33, 494–501.

Bonne, G., Di Barletta, M.R., Varnous, S., Becane, H.M., Hammouda, E.H., Merlini, L., Muntoni, F., Greenberg, C.R., Gary, F., Urtizberea, J.A., Duboc, D., Fardeau, M., Toniolo, D., Schwartz, K., 1999. Mutations in the gene encoding lamin A/C cause autosomal dominant Emery–Dreifuss muscular dystrophy. Nature Genetics 21, 285–288.

Burke, B., Stewart., C.L., 2002. Life at the edge: the nuclear envelope and human disease. Nature Reviews Molecular Cell Biology 3, 575–585.

Caille, N., Thoumine, O., Tardy, Y., Meister, J.J., 2002. Contribution of the nucleus to the mechanical properties of endothelial cells. Journal of Biomechanics 35, 177–187.

Cao, H., Hegele, R.A., 2000. Nuclear lamin A/C R482Q mutation in canadian kindreds with Dunnigan-type familial partial lipodystrophy. Human Molecular Genetics 9, 109–112.

Charras, G.T., Williams, B.A., Sims, S.M., Horton, M.A., 2004. Estimating the sensitivity of mechanosensitive ion channels to membrane strain and tension. Biophysical Journal 87, 2870–2884.

Dahl, K.N., Kahn, S.M., Wilson, K.L., Discher, D.E., 2004. The nuclear envelope lamina network has elasticity and a compressibility limit suggestive of a molecular shock absorber. Journal of Cell Science 117, 4779–4786.

Dahl, K.N., Engler, A.J., Pajerowski, J.D., Discher, D.E., 2005. Power-law rheology of isolated nuclei with deformation mapping of nuclear sub-structures. Biophysical Journal 98, 519–560.

Davies, P.F., 1995. Flow-mediated endothelial mechanotransduction. Physiological Reviews 75, 519–560.

Deguchi, S., Maeda, K., Ohashi, T., Sato, M., 2005. Flow-induced hardening of endothelial nucleus as an intracellular stress-bearing organelle. Journal of Biomechanics 38, 1751–1759.

Dillon, N., 2004. Heterochromatin structure and function. Biology of the Cell 96, 631–637.

Discher, D.E., Boal, D.H., Boey, S.K., 1998. Simulations of erythrocyte cytoskeleton at large deformation. II. Micropipette aspiration. Biophysical Journal 75, 1584–1597.

Drury, J.L., Dembo, M., 1999. Hydrodynamics of micropipette aspiration. Biophysical Journal 76, 110–128.

Eriksson, M., Brown, W.T., Gordon, L.B., Glynn, M.W., Singer, J., Scott, L., Erdos, M.R., Robbins, C.M., Moses, T.Y., Berglund, P., Dutra, A., Pak, E., Durkin, S., Csoka, A.B., Boehnke, M., Glover, T.W., Collins, F.S., 2003. Recurrent de novo point mutations in lamin A cause Hutchinson–Gilford progeria syndrome. Nature 423, 293–298.

Fabry, B., Maksym, G.N., Butler, J.P., Glogauer, M., Navajas, D., Fredberg, J.J., 2001. Scaling the microrheology of living cells. Physical Review Letters 87, 148102–148105.

Fabry, B., Maksym, G.N., Butler, J.P., Glogauer, M., Navajas, D., Taback, N.A., Millet, E.J., Fredberg, J.J., 2003. Time scale and other invariants of integrative mechanical behavior in living cell. Physical Review E 68, 041914.

Fatkin, D., MacRae, C., Sasaki, T., Wolff, M.R., Porcu, M., Frenneaux, M., Atherton, J., Vidaillet, H.J., Spudich, S., De Girolami, U., Seidman, J.G., Seidman, C., Muntoni, F., Muehle, G., Johnson, W., McDonough, B., 1999. Missense mutations in the rod domain of the lamin A/C gene as causes of dilated cardiomyopathy and conduction-system disease. The New England Journal of Medicine 341, 1715–1724.

Fidzianska, A., Toniolo, D., Hausmanowa-Petrusewicz, I., 1998. Ultrastructural abnormality of sarcolemmal nuclei in Emery–Dreifuss muscular dystrophy (EDMD). Journal of Neurological Sciences 159, 88–93.

Flaherty, J.T., Pierce, J.E., Ferrans, V.J., Patel, D.J., Tucker, W.K., Fry, D.L., 1972. Endothelial nuclear patterns in the canine arterial tree with particular reference to hemodynamic events. Circullation Research 30, 23–33.

Guilak, F., Tedrow, J.R., Burgkart, R., 2000. Viscoelastic properties of the cell nucleus. Biochemical and Biophysical Research Communications 269, 781–786.

Guilak, F., Alexopoulos, L.G., Haidar, M.A., Ting-Beall, H.P., Setton, L.A., 2005. Zonal uniformity in mechanical properties of the chondrocyte pericellular matrix: micropipette aspiration of canine chondrons isolated by cartilage homogenization. Annals of Biomedical Engineering 33, 1312–1318.

Haidar, M.A., Guilak, F., 2000. An axisymmetric boundary integral model for incompressible linear viscoelasticity: application to the micropipette aspiration contact problem. Journal of Biomechanical Engineering 122, 236–244.

Haque, F., Lloyd, D.J., Smallwood, D.T., Dent, C.L., Shanaham, C.M., Fry, A.M., Trembath, R.C., Shackleton, S., 2006. SUN1 interacts with nuclear lamin A and cytoplasmic nesprins to provide a physical connection between the nuclear lamina and the cytoskeleton. Molecular and Cellular Biology 26, 3738–3751.

Heinrich, V., Ritchie, K., Mohandas, N., Evans, E., 2001. Elastic thickness compressibility of the red cell membrane. Biophysical Journal 81, 1452–1463.

Hutchison, C.J., Alvarez-Reyes, M., Vaughan, O.A., 2001. Lamins in disease: why do ubiquitously expressed nuclear envelope proteins give rise to tissue-specific disease phenotypes? Journal of Cell Science 114, 9–19.

Ingber, D.E., 1997. Tensegrity: the architectural basis of cellular mechanotransduction. Annual Review of Physiology 59, 575–599.

Janmey, P.A., 1998. The cytoskeleton and cell signaling: component localization and mechanical coupling. Physiological Reviews 78, 763–781.

Lammerding, J., Schulze, P.C., Takahashi, T., Kozlov, S., Sullivan, T., Kamm, R.D., Stewart, C.L., Lee, R.T., 2004. Lamin A/C deficiency causes defective nuclear mechanics and mechanotransduction. Journal of Clinical Investigation 113, 370–378.

Lammerding, J., Hsiao, J., Schulze, P.C.h., Kozlov, S., Stewart, C.L., Lee, R.T., 2005. Abnormal nuclear shape and impaired mechanotransduction in emerin-deficient cells. The Journal of Cell Biology 170, 781–791.

Maraldi, N.M., Lattanzi, G., Marmiroli, S., Squarzoni, S., Manzoli, F.A., 2004. New roles for lamins, nuclear envelope proteins and actin in the nucleus. Advances in Enzyme Regulation 44, 155–172.

McKeon, F.D., Kirschner, M.W., Caput, D., 1986. Homologies in both primary and secondary structure between nuclear envelope and intermediate filament proteins. Nature 319, 463–468.

Mohandas, N., Evans, E., 1994. Mechanical properties of the red cell membrane in relation to molecular structure and genetic defects. Annual Review of Biophysics and Biomolecular Structure 23, 787–818.

Muchir, A., Bonne, G., van der Kooi, A.J., van Meegen, M., Baas, F., Bolhuis, P.A., de Visser, M., Schwartz, K., 2000. Identification of mutations in the gene encoding lamins A/C in autosomal dominant limb girdle muscular dystrophy with atrioventricular conduction disturbances (LGMD1B). Human Molecular Genetics 9, 1453–1459.

Newport, J.W., Forbes, D.J., 1987. The nucleus: structure, function, and dynamics. Annual Review of Biochemistry 56, 535–565.

Ostlund, C., Worman, H.J., 2003. Nuclear envelope Proteins and Neuromuscular diseases. Muscle and Nerve 27, 393–406.

Padmakumar, V.C., Libotte, T., Lu, W., Zaim, H., Abraham, S., Noegel, A.A., Gotzmann, J., Karakesisoglou, I., 2005. The inner nuclear membrane protein Sun1 mediates the anchorage of Nesprin-2 to the nuclear envelope. Journal of Cell Science 118, 3419–3430.

Panorchan, P., Wirtz, D., Tseng, Y., 2004a. Structure-function relationship of biological gels revealed by multiple-particle tracking and differential interference contrast microscopy: the case of human lamin networks. Physical Review E 70, 041906.

Panorchan, P., Schafer, B.W., Wirtz, D., Tseng, Y., 2004b. Nuclear envelope breakdown requires overcoming the mechanical integrity of the nuclear lamina. The Journal of Biological Chemistry 279, 43462–43467.

Pflumm, M.F., 2002. The role of DNA replication in chromosome condensation. BioEssays 24, 411–418.

Rowat, A.C., Foster, L.J., Nielsen, M.M., Weiss, M., Ipsen, J.H., 2005. Characterization of the elastic properties of the nuclear envelope. Journal of The Royal Society Interface 2, 63–69.

Rowat, A. C., Lammerding, J., Ipsen, J. H. 2006. Mechanical properties of the cell nucleus and the effect of emerin deficiency. Biophysical Journal, in press.

Schatten, G., Thoman, M., 1978. Nuclear surface complex as observed with the high resolution scanning electron microscope. Visualization of the membrane surfaces of the nuclear envelope and the nuclear cortex from *Xenopus laevis* oocytes. The Journal of Cell Biology 77, 517–535.

Senda, T., Iizuka-Kogo, A., Shimomura, A., 2005. Visualization of the nuclear lamina in mouse anterior pituitary cells and immunocytochemical detection of lamin A/C by quick-freeze freeze-substitution electron microscopy. Journal of Histochemistry and Cytochemistry 53, 497–507.

Sollich, P., 1998. Rheological constitutive equation for a model of soft glassy materials. Physical Review E 58, 738–759.

Stuurman, N., Mausa, N., Fisher, P.A., 1995. Interphase phosphorylation of the Drosophila nuclear lamin: site-mapping using a monoclonal antibody. Journal of Cell Science 108, 3137–3144.

Swedlow, J.R., Hirano, T., 2003. The making of the mitotic chromosome: modern insights into classical questions. Molecular Cell 11, 557–569.

Trickey, W.R., Lee, G.M., Guilak, F., 2000. Viscoelastic properties of chondrocytes from normal and osteoarthritic human cartilage. Journal of Orthopaedic Research 18, 891–898.

Trickey, W.R., Baaijens, F.P., Laursen, T.A., Alexopoulos, L.G., Guilak, F., 2006. Determination of the Poisson's ratio of the cell: recovery properties of chondrocytes after release from complete micropipette aspiration. Journal of Biomechanics 39, 78–87.

Tseng, Y., Lee, J.S., Kole, T.P., Jiang, I., Wirtz, D., 2004. Micro-organization and visco-elasticity of the interphase nucleus revealed by particle nanotracking. Journal of Cell Science 117, 2159–2167.

Vaziri, A., Lee, H., Kaazempur-Mofrad, M.R., 2006. Deformation of the cell nucleus under indentation: mechanics and mechanisms. Journal of Materials Research 21, 2126–2135.

Vaziri, A., Xue, A., Kamm, R.D., Kaazempur-Mofrad, M.R., 2007. A computational study on cell mechanics based on power-law rheology, Computational Methods in Applied Mechanics and Engineering, in press.

Wilson, K., 2005. Integrity matters: linking nuclear architecture to lifespan. Proceedings of the National Academy of Sciences 102, 18767–18768.

Worman, H.J., Courvalin, J.C., 2004. How do mutations in lamins A and C cause disease? Journal of Clinical Investigation 113, 349–351.

Zhelev, D.V., Needham, D., Hochmuth, R.M., 1994. Role of the membrane cortex in neutrophil deformation in small pipets. Biophysical Journal 67, 696–705.